

# Preventing Biomolecular Adsorption in Electrowetting-Based Biofluidic Chips

Jeong-Yeol Yoon and Robin L. Garrell\*

Department of Chemistry and Biochemistry, and Biomedical Engineering Interdepartmental Program, University of California, Los Angeles, California 90095-1569

**Electrowetting-on-dielectric (EWOD) is a new method for moving liquids in biofluidic chips through electrical modification of the surface hydrophobicity. EWOD-based devices are reconfigurable, have low power requirements, and can handle neutral and charged analytes, as well as particulates. We show that biomolecular adsorption in EWOD is minimized by limiting the time during which no potential is applied and through choice of solution pH and electrode polarity. The same approach may be useful for controlling biomolecular adsorption in other applications of hydrophobic dielectric materials. These results demonstrate the feasibility of implementing EWOD for fluid actuation in biofluidic chips.**

Electrowetting-on-dielectric (EWOD) is a new method for moving liquids in lab-on-a-chip devices, such as biofluidic chips. In EWOD, a droplet of liquid rests on a surface or in a channel coated with a hydrophobic, insulating (dielectric) material. The surface is modified from hydrophobic to hydrophilic by applying a voltage between the liquid and an electrode under the dielectric layer,<sup>1–3</sup> as illustrated in Figure 1. Charge accumulates at the solid–liquid interface, leading to a change in wettability from hydrophobic to hydrophilic and a decrease in the liquid–solid contact angle. Equation 1 is the Young–Lippmann equation, which shows the relationship between contact angle and applied voltage.<sup>4</sup>

$$\cos \theta_V = \cos \theta_0 + \frac{1}{2} \frac{\epsilon \epsilon_0}{\gamma_{LV} d} V^2 \quad (1)$$

Here,  $\theta_V$  is the contact angle when a potential is applied,  $\theta_0$  the contact angle in the absence of an applied potential,  $\epsilon$  the dielectric constant of a dielectric layer,  $\epsilon_0$  the dielectric constant of air,  $\gamma_{LV}$  the surface tension of the liquid–vapor interface,  $d$  the thickness of the dielectric layer, and  $V$  the applied voltage. A smaller thickness  $d$  or larger dielectric constant  $\epsilon$  allows a larger contact angle change to be obtained at a given applied voltage. The lowest voltage for EWOD actuation reported to-date is 15 V for a 40° contact angle change.<sup>4</sup>

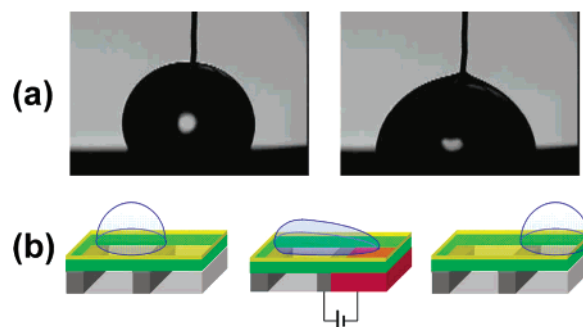


Figure 1. (a) A 5- $\mu$ L aqueous BSA droplet on Teflon AF-coated SiO<sub>2</sub>/silicon, before and while applying a  $-30\text{-V}_{\text{dc}}$  potential across the droplet. (b) Illustration of fluid motion induced by applying an electrical potential across dielectric-coated electrodes below a liquid droplet. By switching on the voltage at an electrode adjacent to the droplet, the surface tension is lowered, causing the droplet to move to the right. The droplet returns to its original shape when the potential is switched off.

By applying a sequence of voltages to electrodes patterned under the dielectric layer, it is possible to create droplets from a reservoir<sup>5</sup> and to move,<sup>6–8</sup> cut, and join them.<sup>5,7</sup> An EWOD-based biofluidic chip is shown schematically in Figure 2a. Droplets are ejected from sample and reagent reservoirs and programmed to move to specific locations where they can be merged and interrogated, electrochemically or optically. The analysis scheme may or may not involve reaction of the sample with immobilized reagents. The creation, movement, and joining of droplets are demonstrated in Figure 2b.<sup>9</sup>

There are three principal advantages to using EWOD for micro- and nanoscale biofluidics. First, it is very general; unlike electrophoresis or dielectrophoresis, it does not require the soluble or particulate analytes to be charged or to have large polarizabilities.<sup>6</sup> Second, the power required to transport liquid is much lower than in pumping- or electrophoresis-based devices.<sup>10,11</sup> Third, an EWOD-based device can be reconfigured simply by reprogram-

\* Corresponding author. Fax: 310-206-2061. E-mail: garrell@chem.ucla.edu.

(1) Vallet, M.; Berge, B.; Vovelle, L. *Polymer* **1996**, *37*, 2465–2470.

(2) Vallet, M.; Vallade, M.; Berge, B. *Eur. Phys. J. B* **1999**, *11*, 583–591.

(3) Berge, B.; Peseux, J. *Eur. Phys. J. E* **2000**, *3*, 159–163.

(4) Moon, H.; Cho, S. K.; Garrell, R. L.; Kim, C.-J. *J. Appl. Phys.* **2002**, *92*, 4080–1087.

(5) Cho, S. K.; Fan, S.-K.; Moon, H.; Kim, C.-J. *IEEE Conf. Micro Electro Mech. Syst.*, Las Vegas, NV, 2002; pp 32–35.

(6) Lee, J.; Moon, H.; Fowler, J.; Schoellhammer, T.; Kim, C.-J. *Sens. Actuators, A* **2002**, *95*, 259–268.

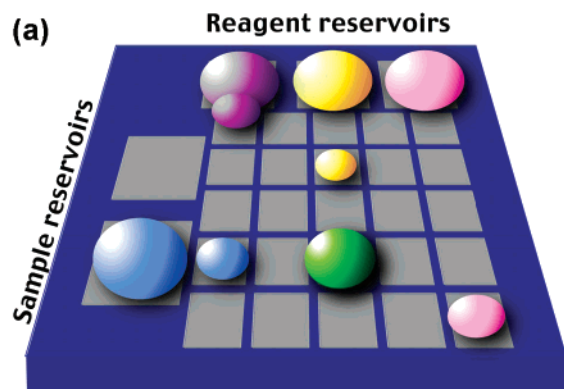
(7) Pollack, M. G.; Shenderov, A. D.; Fair, R. B. *Lab Chip* **2002**, *2*, 96–101.

(8) Ding, J.; Chakrabarty, K.; Fair, R. B. *IEEE Trans. Comput.-Aided Des.* **2001**, *20*, 1463–1468.

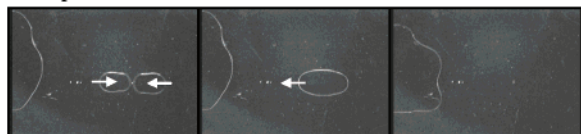
(9) Fan, S.-K.; Hashi, C.; Kim, C.-J. *IEEE Conf. Micro Electro Mech. Syst.*, Kyoto, Japan, 2003; pp 694–697.

(10) Lee, J.; Kim, C.-J. *J. Microelectromech. Syst.* **2000**, *9*, 171–180.

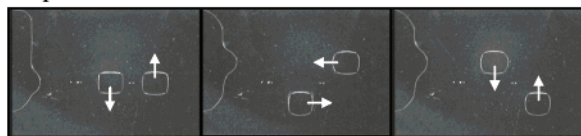
(11) Quilliet, C.; Berge, B. *Curr. Opin. Colloid Interface Sci.* **2001**, *6*, 34–39.



A single droplet is created from a reservoir and split into 2 droplets.



Independent and simultaneous transportation of two droplets.



Merging of two droplets and returning to the reservoir.

Figure 2. (a) Schematic illustration of EWOD-based biofluidic chip, in which sample and reagent droplets can be created and moved to specific sites in the array. The device is reconfigured simply by reprogramming the sequence of applied voltages used to create, move, join, and divide the droplets. (For clarity, the transparent top electrode is not shown.) (b) Creating, moving, and merging droplets in a EWOD-based microfluidic chip. Reprinted from ref 9 with permission (copyright 2003 IEEE).

ming the sequence of applied potentials.<sup>12</sup> Because the liquid is not in direct contact with the electrodes, as they would be in ordinary electrowetting, electrolysis and analyte redox reactions are avoided, enhancing device stability.<sup>6</sup>

One of the biggest challenges for all biofluidic chips, including those operated by EWOD, is preventing nonspecific adsorption of biomolecules. Proteins and other biomolecules adsorb from aqueous solutions onto hydrophobic surfaces such as Teflon<sup>13–15</sup> and poly(dimethylsiloxane)<sup>16,17</sup> through hydrophobic interactions.

(12) Fan, S.-K.; de Guzman, P.-P.; Kim, C.-J. *Solid-State Sensor Actuator Microsystem Workshop*, Hilton Head Island, SC, 2002; pp 134–137.

(13) Absolom, D. R.; Zingg, W.; Neumann, A. W. *J. Biomed. Mater. Res.* **1987**, *21*, 161–171.

(14) Makohliso, S. A.; Giovangrandi, L.; Léonard, D.; Mathieu, H. J.; Ilegems, M.; Aebischer, P. *Biosens. Bioelectron.* **1998**, *13*, 1227–1235.

(15) van der Wegt, W.; Norde, W.; van der Mei, H. C.; Busscher, H. J. *J. Colloid Interface Sci.* **1996**, *179*, 57–65.

(16) Rakhorst, G.; van der Mei, H. C.; van Oeveren, W.; Spijker, H. T.; Busscher, H. J. *Int. J. Artif. Organs* **1999**, *22*, 35–39.

(17) Kim, Y.-D.; Park, C. B.; Clark, D. S. *Biotechnol. Bioeng.* **2001**, *73*, 331–337.

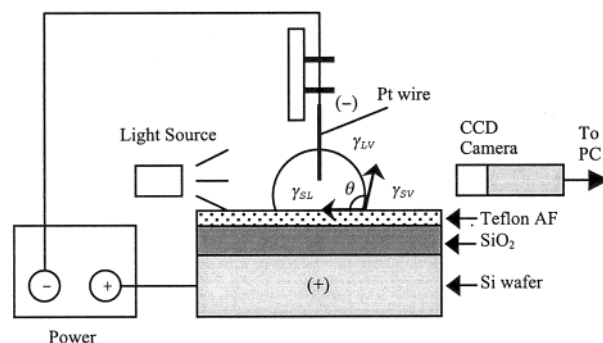


Figure 3. Experimental arrangement for measuring voltage-induced contact angle changes in droplets on dielectric-coated electrodes.

Applying a potential can cause biomolecules to adsorb through electrostatic attractions. Adsorption arising from either hydrophobic or electrostatic interactions can perturb the contact angle and will ultimately degrade the device performance.

The feasibility of manipulating biofluids in contact with silicone oil by EWOD has recently been demonstrated.<sup>18</sup> Potential concerns with using oil as the ambient medium include the possibility of protein adsorption and entrapment (emulsification) at the water–oil interface<sup>19</sup> and the higher power needed to manipulate droplets in a viscous oil medium compared to air.<sup>18</sup>

In this paper, we describe methods to minimize biomolecular adsorption in EWOD-based fluid actuation in air-filled channels.<sup>20</sup> The substrates consisted of 500-Å Teflon AF (amorphous fluoropolymer) spin-coated onto 1200-Å SiO<sub>2</sub> on silicon, which we have shown provides highly reversible electrowetting for water with an applied voltage less than 30 V and with no electrolysis.<sup>4,21</sup> As model biofluids, we examined aqueous solutions of bovine serum albumin (BSA), hen egg white lysozyme, and calf thymus DNA, as well as adult bovine whole serum. The behavior of droplets in EWOD-based devices was modeled by depositing a 5-μL droplet onto the substrate, inserting a 0.1-mm-diameter Pt electrode, and applying constant or square wave potentials. The contact angle was monitored in real time with an FTÅ 4000 contact angle goniometer, as shown in Figure 3. It will be shown that, by choosing the solution pH and the square wave parameters, biomolecule adsorption on the hydrophobic surface can be minimized or eliminated. This strategy may be generally applicable for minimizing biomolecular adsorption on hydrophobic surfaces.

## EXPERIMENTAL SECTION

**Reagents and Materials.** Protein solutions were made from BSA (P-7656, Sigma, St. Louis, MO) and hen egg white lysozyme (L-6876, Sigma). The isoelectric point (pI) of BSA is 4.7, and of lysozyme, 10.7.<sup>22</sup> Double-stranded deoxyribonucleic acid from calf thymus (sodium salt, D-3664, Sigma) was used as a model DNA. Adult bovine whole serum (B-2771, Sigma) was used as an example of a complex biofluid. Protein concentrations were

(18) Srinivasan, V.; Pamula, V.; Pollack, M.; Fair, R. B. *IEEE Conf. Micro Electro Mech. Syst.*, Kyoto, Japan, 2003; pp 327–330.

(19) Bartzoka, V.; Brook, M. A.; McDermott, M. R. *Langmuir* **1998**, *14*, 1887–1891.

(20) Felton, M. *Anal. Chem.* **2002**, *74*, 517A.

(21) Saeki, F.; Baum, J.; Moon, H.; Yoon, J.-Y.; Kim, C.-J.; Garrell, R. L. *Polym. Mater. Sci. Eng.* **2001**, *85*, 12–13.

(22) Luo, Q. L.; Andrade, J. D. *J. Colloid Interface Sci.* **1998**, *200*, 104–133.

quantified by Bradford assay using Bio-Rad dye reagent concentrate (Bio-Rad Lab., Hercules, CA). The total biomolecule concentration was 4  $\mu\text{g/mL}$  in all cases. Acetate buffer was prepared from acetic acid and sodium acetate (Fisher, Fair Lawn, NJ). The ionic strength of the acetate buffer was 0.001. pH was measured by colorpHast pH indicator strips (EM Science, Cherry Hill, NJ), with an accuracy of  $\pm 0.1$ . Water was from a Millipore Super-Q system (Bedford, MA), pH 6.5.

**Substrates.** The substrates consisted of 1200-Å  $\text{SiO}_2$  grown on a silicon wafer by thermal oxidation. To make the surface hydrophobic, 500 Å of Teflon AF (poly(tetrafluoroethylene-co-2,2-bis(trifluoromethyl)-4,5-difluoro-1,3-dioxane, DuPont, Wilmington, DE) was spin-coated onto the  $\text{SiO}_2$  layer.<sup>4</sup> Teflon AF was diluted from 6 (as received from DuPont) to 0.6% with Fluorinert FC 75 (3M, St. Paul, MN) to achieve the desired thickness. All thicknesses were quantified by ellipsometry (Gaertner L116B ellipsometer, Skokie, IL).

**Apparatus.** A  $-30\text{-V}_{\text{dc}}$  potential was applied using a dc power supply from Tektronix (Beaverton, OR). The 0.1-Hz square wave of  $\pm 30\text{-V}_{0-p}$  potential (oscillating from 0 to +30 V or from 0 to  $-30\text{ V}$ , for 10 s) was generated by a Tektronix CFG253 function generator (Beaverton, OR) and amplified by a Trek model 603 power amplifier/piezodriver (Medina, NY). The waveform was tested by the manufacturer (Trek Inc.). The electrical current was monitored by a Keithley model 169 digital multimeter (Cleveland, OH). Contact angles were evaluated with an FTÅ 4000 Micro-drop contact angle goniometer (First Ten Ångströms, Portsmouth, VA), capturing 3 frames  $\text{s}^{-1}$ . A 0.1-mm platinum wire (99.99%, Aldrich, Milwaukee, WI) was inserted into the droplet. A tungsten probe contacted the bottom (silicon) layer, as shown in Figure 2. Unless otherwise stated, a negative potential ( $-30\text{ V}$ ) was applied to the droplet and positive potential to the bottom layer. All experiments were performed at  $23 \pm 1\text{ }^\circ\text{C}$  and  $48 \pm 2\%$  relative humidity.

There was no apparent electrolysis or measurable electric current between the Pt electrode and the TeflonAF/ $\text{SiO}_2$ -coated Si substrate upon applying  $\pm 30\text{-V}$  potentials, indicating the combined dielectric layer behaved as an insulator and did not undergo dielectric breakdown. (The double-layer charging current was too small to detect in this experimental arrangement.<sup>23</sup>) By contrast, the same experiment on substrates consisting of thin Teflon AF on silicon with no intermediate  $\text{SiO}_2$  layer produced a large number of bubbles.

**Quartz Crystal Microbalance (QCM) Experiments.** As an independent assay of biomolecular adsorption onto Teflon AF, we performed QCM experiments. For these experiments, 500-Å Teflon AF was spin-coated on one side of a polished 9-MHz AT-cut quartz crystal resonator (International Crystal Manufacturing, Oklahoma City, OK). The resonance frequency,  $f$ , was measured with an impedance analyzer (Hewlett-Packard, now Agilent, model 4192A, Agilent Technologies, Inglewood, CO) before and immediately after depositing a 5- $\mu\text{L}$  droplet of either pure water or 4  $\mu\text{g/mL}$  BSA solution in the center of the Teflon-coated face of the resonator. A 0.1-mm Pt electrode was inserted into the droplet. A  $-30\text{-V}_{\text{dc}}$  potential was applied for 2 min, and then the top electrode was removed from the droplet and the resonance frequency remeasured. In most experiments, no electrolysis was observed; data for the occasional instances when a small amount

of electrolysis did occur are not included here. (Because the  $-30\text{-V}_{\text{dc}}$  potential on the inserted electrode interfered with determining the resonance frequency by the impedance analyzer, the electrode had to be removed for the frequency measurement.) The contact angle was preserved after electrode emersion; i.e., there was no redistribution of the accumulated charge. This was confirmed by control experiments with water on silicon/ $\text{SiO}_2$ /Teflon AF substrates, in which  $\theta$  was shown to drift only  $2^\circ$  over 10 min following electrode emersion. Reinserting the electrode had no effect on the contact angle; it only changed when a different potential was applied. The change in frequency before and after the applied potential,  $\Delta f$ , represents the combined effects of adsorption on the resonator surface (mass loading) and changing the liquid–solid contact area (wetting).<sup>26</sup>

## RESULTS AND DISCUSSION

**Passive Biomolecular Adsorption.** It is well known that proteins readily and irreversibly adsorb on hydrophobic surfaces such as Teflon.<sup>13–15</sup> To determine the extent of this “passive” biomolecular adsorption (i.e., fouling in the absence of an applied potential), we deposited droplets onto the Teflon AF substrate and monitored the contact angle over time with no applied potential. Contact angle is commonly used as an assay of biomolecular adsorption inside a sessile droplet.<sup>15,16,27–31</sup> The results are shown in Figure 4. In 10 min, the contact angle decreased  $2^\circ$  for water (due to pinning of the contact line during

(23) The double-layer charging current can be estimated for the combined Teflon AF/ $\text{SiO}_2$  dielectric by treating it as a capacitor whose total capacitance,  $C$ , can be calculated from  $C = \epsilon_0 \epsilon_r A / d$  and  $1/C = \sum_i 1/C_i$  (1). Here,  $\epsilon_0$  is the permittivity of a free space ( $8.85 \times 10^{-12} \text{ F}\cdot\text{m}^{-1}$ ),  $\epsilon_r$  is the dielectric constant of the material (1.9 for Teflon AF and 3.8 for  $\text{SiO}_2$ ),<sup>24</sup>  $A$  is the electrode area, and  $d$  is the distance between electrodes. Using for  $A$  the contact area of a 5- $\mu\text{L}$  droplet (5.61 mm<sup>2</sup>, measured with the FTÅ4000), 500 Å for  $d$  of Teflon, and 1200 Å for  $d$  of  $\text{SiO}_2$ , the total capacitance is calculated as 0.86 nF. Upon applying a  $-30\text{-V}$  potential, current will flow until the capacitor is fully charged (charging current). Charge will accumulate at the Teflon–water and  $\text{SiO}_2$ –Si interfaces. The current ( $I$ ) can be calculated from:  $I = V/R_s \exp(-t/R_s C_d)$  (2), where  $R_s$  is the solution resistance and  $C_d$  is the double-layer capacitance, assumed equal to the total capacitance,  $C$ , above. The resistivity of our deionized water was 3.00  $\text{M}\Omega\cdot\text{cm}$  (YSI 3200 conductivity meter, YSI, Yellow Springs, OH). The distance between the Pt wire and bottom substrate was 0.668 mm, (measured with the FTÅ4000). The corresponding cell constant (the ratio of the distance between the electrodes to the area normal to the current flow) was  $1.191 \text{ cm}^{-1}$ . Under these conditions, the calculated capacitive current is 90 nA at  $t = 14\text{ ms}$ , and less than 1 nA at 28 ms. For the 1 mM pH 4.0 acetate buffer,  $R_s$  was 24.5  $\text{k}\Omega\cdot\text{cm}$ ; the resulting capacitive current would be less than 1 nA at  $t > 0.4\text{ ms}$ . The resistivity of a 4  $\mu\text{g/mL}$  protein solution and the resulting capacitive current should be intermediate between those of deionized water and 1 mM acetate buffer. Because the detection limit and time resolution of the multimeter used in these experiments (Keithley model 169) are 100 nA and 100 ms, respectively, these tiny capacitive currents would not be detectable.

- (24) Rampi, M. A.; Schueller, O. J. A.; Whitesides, G. M. *Appl. Phys. Lett.* **1998**, *72*, 1781–1783.
- (25) Ding, S.-J.; Wang, P.-F.; Zhang, D. W.; Wang, J.-T.; Lee, W. W. *Mater. Lett.* **2001**, *49*, 154–159.
- (26) Teuscher, J. H.; Yeager, L. J.; Yoo, H.; Chadwick, J. E.; Garrell, R. L. *Faraday Discuss.* **1997**, *107*, 399–416.
- (27) Davies, J.; Nunnerley, C. S.; Brisley, A. C.; Edwards, J. C.; Finlayson, S. D. *J. Colloid Interface Sci.* **1996**, *182*, 437–443.
- (28) Grundke, K.; Werner, C.; Poschel, K.; Jacobasch, H. J. *Colloids Surf. A* **1999**, *156*, 19–31.
- (29) do Serro, A. P. V. A.; Fernandes, A. C.; Saramgo, B. J. V.; Norde, W. J. *Biomed. Mater. Res.* **1999**, *46*, 376–381.
- (30) Koopal, L. K.; Goloub, T.; de Keizer, A.; Sidorova, M. P. *Colloids Surf. A* **1999**, *151*, 15–25.
- (31) Haynes, C. A.; Norde, W. *Colloids Surf. B* **1994**, *2*, 517–566.



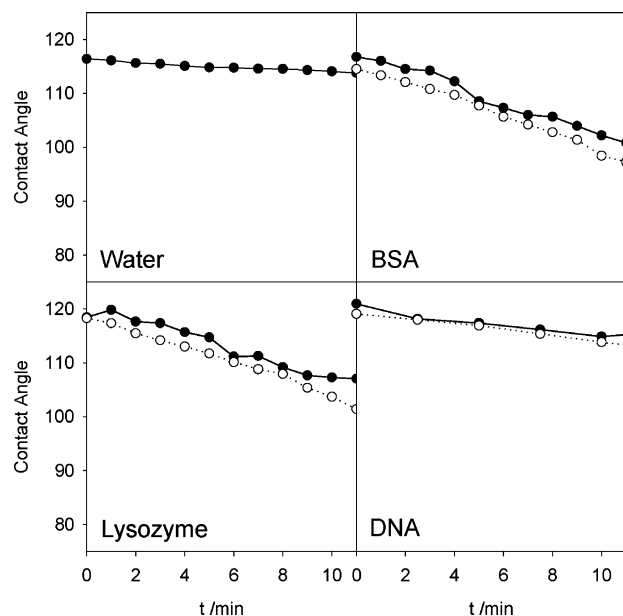


Figure 4. Contact angle changes for BSA, lysozyme, and DNA solutions on Teflon AF with no applied potential. Filled symbols (●) in water (pH 6.5); open symbols (○) in pH 7.2 phosphate buffer (ionic strength 0.001).

evaporation, primarily because of surface roughness or heterogeneity<sup>32</sup>), 15° for the BSA solutions, 13–17° for the lysozyme solutions, and 6° for the DNA solutions. While the contact angle drifted for all the biomolecule solutions, the change was significantly larger for the protein solutions than for DNA, indicating more extensive passive adsorption on the hydrophobic surface.<sup>15,27–29</sup>

**Effect of Electrode Polarity on EWOD.** Figure 5a illustrates the electrical charge on BSA and lysozyme as a function of pH. At pH 6.5 (pure water) or pH 7.2 (phosphate buffer), both BSA and DNA are negatively charged, while lysozyme is positively charged. When a  $-30\text{-V}_{\text{dc}}$  potential is applied (i.e., negative bias on the inserted electrode, positive bias on the substrate), BSA and DNA will be electrostatically attracted to the substrate, while lysozyme will be repelled, as illustrated in Figure 5b. We first determined how the electrode polarity affects the magnitude of the potential-induced contact angle change. Figure 6 shows the contact angle as a function of time when a  $-30\text{ V}_{\text{dc}}$  was applied to BSA, DNA, and lysozyme solutions in water (pH 6.5) and phosphate buffer (pH 7.2). No significant differences were found between the behavior of these three analytes in water versus buffer solution. When the voltage was turned on, the contact angle for the lysozyme solution was about the same as that for pure water ( $\sim 83^\circ$ ); because the lysozyme was positively charged, it did not adsorb on the positively charged surface. The BSA and DNA solutions showed larger contact angles than water when the voltage was applied:  $\sim 87\text{--}89^\circ$ . If the negatively charged BSA and DNA were to electrostatically adsorb on the positively charged substrate, as illustrated in Figure 5b, the effective thickness of the dielectric would increase. According to eq 1, this would decrease  $\cos \theta_V$  and increase  $\theta_V$  at that voltage, as we observed.

We then determined how the electrode polarity affects the EWOD reversibility, through applying  $-30$  or  $+30\text{ V}_{0\text{-p}}$  square wave potentials at 0.1 Hz (oscillating from 0 to  $-30/+30\text{ V}$  every

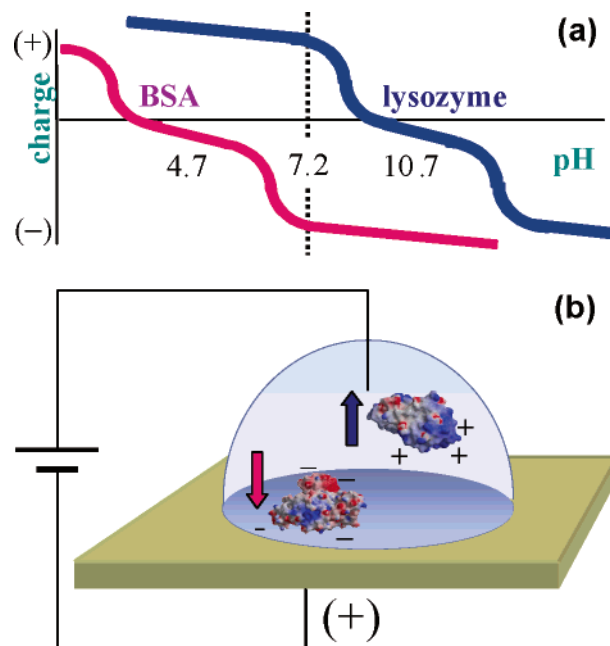


Figure 5. (a) Schematic illustration of the charge on BSA and lysozyme as a function of pH; (b) electrostatically driven protein adsorption at pH 7.2. The negatively charged BSA is shown migrating to the anode and positively charged lysozyme migrating to the cathode. Lysozyme and BSA are depicted as 2-D topographic surfaces calculated and depicted with the GRASP program;<sup>30</sup> red indicates regions of negative charge and blue regions of positive charge. Protein structures from the Protein Data Bank.<sup>31</sup>

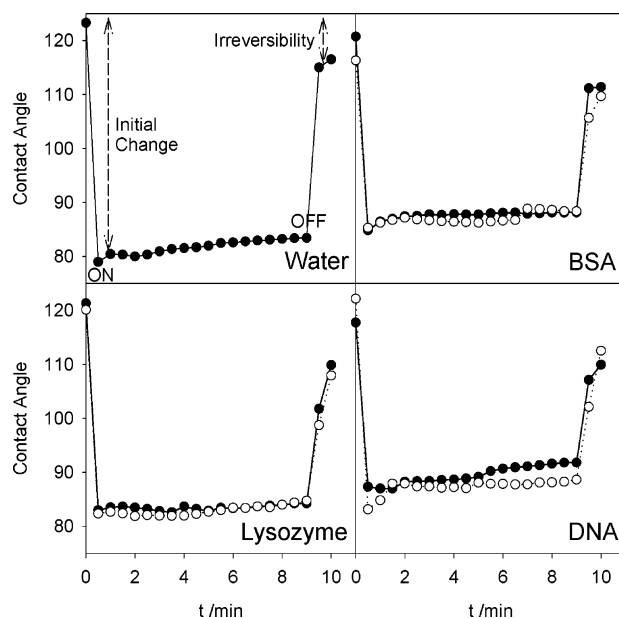


Figure 6. Contact angle changes for BSA, lysozyme, and DNA solutions when a  $-30\text{-V}_{\text{dc}}$  potential was applied at 0.5 min and turned off at 9.5 min. Filled symbols (●) correspond to solutions in water (pH 6.5), open symbols (○) to solutions in pH 7.2 phosphate buffer (ionic strength 0.001).

10 s) to pH 6.5 solutions. This simulates the voltage modulation that is used to move droplets in EWOD-based biofluidic chips. Figure 7 depicts representative results for 10 cycles. Completely reversible wetting and dewetting would represent ideal behavior. We performed at least three experiments for each case and found a maximum variation of  $\pm 5^\circ$  between experiments. With  $-30\text{ V}_{0\text{-p}}$

(32) Hu, H.; Larson, R. G. *J. Phys. Chem. B* **2002**, *106*, 1334–1344.

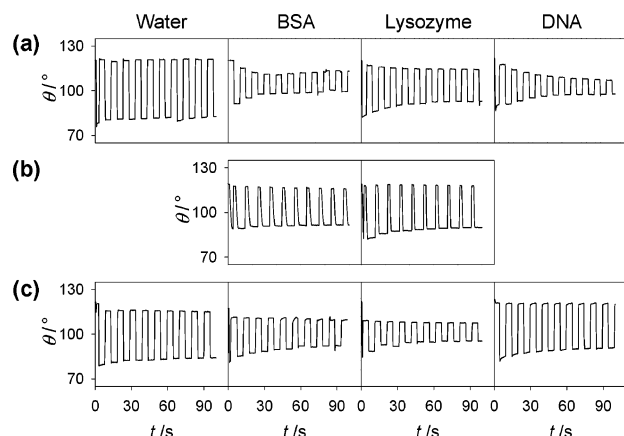


Figure 7. Contact angle changes for BSA, lysozyme, and DNA solutions with  $\pm 30$ -V<sub>0-p</sub> square wave potentials at 0.1 Hz: (a) 5 s at 0 V, 5 s at -30 V; (b) 1 s at 0 V, 9 s at -30 V; (c) 5 s at 0 V, 5 s at +30 V.

(series a, top row), the voltage-induced change in contact angle for all three protein solutions was smaller than for water and decreased over time. These trends are evidence for protein adsorption (surface fouling). This pattern was more pronounced for the BSA and DNA than for the lysozyme solutions. The trend reversed when the polarity was switched to +30 V<sub>0-p</sub> (series c, bottom row). The behavior of BSA with -30 V<sub>0-p</sub> was similar to that of lysozyme with +30 V<sub>0-p</sub> and vice versa. This suggests that protein adsorption in this experiment was primarily electrostatically driven. At pH 6.5, both BSA and DNA are negatively charged; at -30 V<sub>0-p</sub>, they are attracted to the positively charged surface, while positively charged lysozyme is repelled, as suggested in Figure 5.

**Evidence for Electrostatically Driven Biomolecular Adsorption.** To confirm that electrostatically driven biomolecular adsorption occurs, we used a QCM to detect protein adsorption from water onto Teflon AF-coated gold under EWOD conditions. When a polished thickness shear mode quartz crystal resonator is in contact with an aqueous protein solution, both mass loading and changes in adlayer or solution viscosity near the gold electrode (within 0.2  $\mu\text{m}$  for a 9-MHz crystal in aqueous solution) can lead to a shift ( $\Delta f$ ) in the resonance frequency.<sup>35-37</sup> We measured the resonance frequency  $f$  before and after applying a -30-V<sub>dc</sub> potential for 2 min to a droplet placed in the center of the 9-MHz resonator. For the droplet of pure water,  $\Delta f$  was  $219 \pm 32$  Hz (average of four experiments), arising from the change in contact area upon electrowetting.<sup>29</sup> For the 4  $\mu\text{g/mL}$  BSA droplet,  $\Delta f$  was  $504 \pm 99$  Hz (average of two experiments), as a result of the combined effects of electrowetting and protein adsorption. The  $p$ -value was 0.0044, indicating a statistically significant difference in the  $\Delta f$  values for water and the protein solution. If we assume that 100% of the protein in the 5- $\mu\text{L}$  droplet

(20 ng) adsorbed, forming a rigid adlayer,  $\Delta f$  calculated from the Sauerbrey equation would be only 65 Hz. The actual difference of 285 Hz between the  $\Delta f$  values for water and the protein solution is thus attributable to the combined effects of mass loading and viscosity changes at the interface associated with protein adsorption. This experiment confirms that applying a potential can indeed induce protein adsorption.

We have thus far identified two mechanisms for biomolecular adsorption under EWOD conditions: passive adsorption arising from hydrophobic interactions and electrostatically driven adsorption when an external electric field is applied. In the next two sections, we show how both problems can be minimized and reversible electrowetting with biofluids achieved.

**Minimizing Passive Biomolecular Adsorption.** At +30 V<sub>0-p</sub> (Figure 7c, bottom row), the DNA solution behaved almost like pure water. It showed a larger contact angle change and better reversibility than the BSA solution, even though both DNA and BSA were negatively charged under those conditions. This indicates factors other than electrostatics contribute to biomolecular adsorption. From the results presented in the previous section, we know that proteins exhibit more extensive passive adsorption than DNA does. The poorer reversibility for protein than DNA solutions in the electrowetting experiment (Figure 7a and c) can thus be understood as arising from adsorption during the portion of the square wave when the applied potential was zero.

To minimize passive biomolecular adsorption, hydrophobic interactions between the biomolecules and surface need to be reduced. One approach would be to use a surface that is less hydrophobic than Teflon AF, but this would make EWOD-based actuation more difficult. An option for biomolecules that exhibit a "salting-in" effect is to increase the ionic strength of the solution. A salting-out effect is more common, however, and that is what we observed for these solutions. Increasing the ionic strength led to irreversible contact angle changes and increased electrolysis (data not shown). As an alternative, we reduced the duration in the square wave during which no potential was applied, specifically, by applying an asymmetric square wave consisting of 1 s at 0 V and 9 s at -30 V. As shown in Figure 7b (middle row), both the BSA and lysozyme solutions showed larger and more reversible contact angle changes than with symmetric square waves (series a and c). It thus appears possible to minimize both passive, hydrophobicity driven and active, electrostatically driven biomolecular adsorption on fluoropolymer surfaces. In real EWOD-based devices, droplets would typically be moved very rapidly, so minimizing contact time would not place any significant limitations on device function. Of course, if a particular path in the device does get contaminated, alternative paths in the reconfigurable device could be utilized.

**Results with Complex Biofluids.** To determine the feasibility of using EWOD to manipulate complex, real-world biofluids, we measured the contact angle reversibility for adult bovine whole serum and for a 1:1 (w/w) mixture of BSA and lysozyme. To minimize both electrostatic and hydrophobic interactions between the solutes and substrate, we used a pH 4.0 acetate buffer, in which most of the proteins would be positively charged, and a -30-V<sub>0-p</sub> square wave (positive bias at substrate). As shown in Figure 8 (representative results from three experiments), both the binary

(33) Nicholls, A.; Sharp, K. A.; Honig, B. *Proteins: Struct. Funct. Genet.* **1991**, *11*, 281-296.

(34) Berman, H. M.; Westbrook, J.; Feng, Z.; Gilliland, G.; Bhat, T. N.; Weissig, H.; Shindyalov, I. N.; Bourne, P. E. *Nucleic Acids Res.* **2000**, *28*, 235-242.

(35) Kanazawa, K. K.; Gordon, J. G. *Anal. Chem.* **1985**, *57*, 1770-1771.

(36) Nimeri, G.; Fredriksson, C.; Elwing, H.; Liu, L.; Rodahl, M.; Kasemo, B. *Colloids Surf. B* **1998**, *11*, 255-264.

(37) Kaspar, M.; Stadler, H.; Weiss, T.; Ziegler, Ch. *Fresenius J. Anal. Chem.* **2000**, *366*, 602-610.

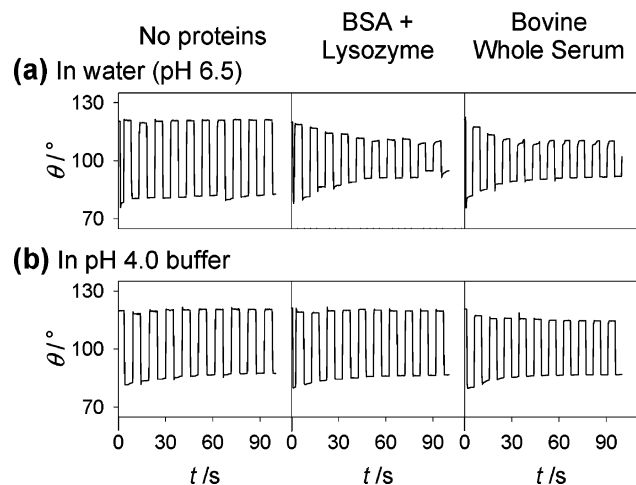


Figure 8. Contact angle changes for BSA + lysozyme (each  $2 \mu\text{g}/\text{mL}$ ) and adult bovine whole serum (total protein concentration  $4 \mu\text{g}/\text{mL}$ ) dissolved in (a) water (pH 6.5) and (b) pH 4.0 acetate buffer (ionic strength 0.001). The potential was a symmetric  $-30\text{-}V_{0-p}$  square wave at 0.1 Hz (5 s at 0 V, 5 s at  $-30$  V).

protein mixture and adult bovine whole serum showed large, nearly reversible contact angle changes in the pH 4.0 buffer (bottom row). The reversibility in this buffer was much better than in deionized water at pH 6.5 (top row), pH 4.7 acetate buffer, or pH 7.2 phosphate buffer (data not shown).

**Consequences of Protein Adsorption.** If proteins adsorb from solution and are left behind on the substrate, they may trigger further protein adsorption and perturb electrowetting by droplets that are subsequently directed to that site. To test this idea, we allowed a  $5\text{-}\mu\text{L}$  droplet of  $4 \mu\text{g}/\text{mL}$  BSA (pH 6.5) to passively foul the fluoropolymer surface for 6.5 min. We then applied a  $-30\text{-}V_{\text{dc}}$  potential for 9 min. As shown in Figure 9 (■), the contact angle decreased during the prepotential period, indicating fouling occurred. Although it was still possible to induce a large contact angle change when the potential was switched on, the contact angle continued to drift downward throughout the 9 min, and the changes could not be reversed when the potential was turned off. By contrast, in the control experiment with no prefouling (●), there was no drift and the contact angle change was almost completely reversible. We interpret these results as evidence that the protein-fouled surface is more susceptible to further protein adsorption than the clean surface and that

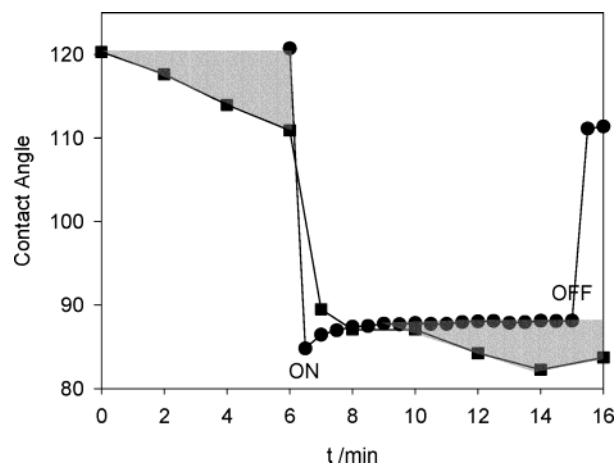


Figure 9. Contact angle change for aqueous BSA on Teflon AF: (■) with no applied potential for 6.5 min, then  $-30\text{-}V_{\text{dc}}$  for 9 min, and then turned off for 0.5 min; (●) with a  $-30\text{-}V_{\text{dc}}$  applied immediately and for 9 min and then turned off for 0.5 min.

extensive protein adsorption leads to completely irreversible electrowetting.

## CONCLUSIONS

We have demonstrated the feasibility of implementing EWOD for fluid actuation in biofluidic chips. Through careful choice of the bias, magnitude, and duration of the applied voltage, the surface wettability can be controlled while minimizing biomolecular adsorption. We are applying these strategies in developing EWOD-based biofluidic chips. The same approach may be useful for controlling biomolecular adsorption in other applications of hydrophobic dielectric materials.

## ACKNOWLEDGMENT

The authors thank Professor Chang-Jin "CJ" Kim, Mr. Brian R. Baker, and Dr. Fusayo Saeki at the University of California, Los Angeles (UCLA), for helpful discussions, and Mr. Keiki Sugimoto at UCLA for providing the GRASP structures. This work was supported by DARPA Contract N66001-00-C-8081 and CMISE, the UCLA Cell Mimetic Institute of Space Exploration (NASA Contract NCC 2-1364).

Received for review March 17, 2003. Accepted July 14, 2003.

AC0342673